Himalaya, dynamics of a giant

Volume 1 - Geodynamic setting of the Himalayan range

Coordinated by Rodolphe CATTIN and Jean-Luc EPARD

September 6, 2023

5

Gravity observations and models along the Himalayan arc

Rodolphe CATTIN[1], György HETÉNYI[2], Théo BERTHET[3] and Jamyang CHOPHEL[4]

[1] *Geosciences Montpellier, University of Montpellier, Montpellier, France*
[2] *Institute of Earth Sciences, University of Lausanne, Lausanne, Switzerland*
[3] *Department of Earth Sciences, Uppsala University, Uppsala, Sweden*
[4] *Earthquake & Geophysics Division, Department of Geology & Mines, Thimphu, Bhutan*

Introduction

In 1823 George Everest was appointed as superintendent of the Indian Geodetic Survey. During his field campaigns in northern India, he noticed that his gravity measurements led to a surprising conclusion: the Himalayan range is associated with a gravity anomaly that could only be explained by a mass deficiency. This result suggests that this mountain had a much lower density than the surface rocks. Far from being erroneous, his measurements confirmed observations made a century earlier in the Andes: "*Pour revenir aux observations faites sur le Chimborazo, il paraît assez*

Himalaya, dynamics of a giant,
coordinated by Rodolphe CATTIN and Jean-Luc EPARD.

qu'on peut dire en se refermant sur le fait simple, que les montagnes agissent en distance, mais que leur action est bien moins considérable que le promet la grandeur de leur volume" [1] (Bouguer 1749).

Since these first discoveries, the amount and quality of gravity measurements along the Himalayan range have continuously increased. Hundreds of gravity field measurements on land (see compilation presented by Hetényi et al. 2016) as well as thousands of space gravity gradiometry [2] data are now available. Together, these observations improve the density distribution assessment under the Himalayan range and thus better define the three-dimensional geometry of Himalayan and Tibetan lithospheric structures.

In this chapter, after a brief presentation of gravity methods and corrections, we go through the main isostasy models. Next, we show how land gravity measurements are used to explain the mechanical support of the Himalayan topography, characterized by a spatial extension of ∼2,400 km in length and peaks exceeding 8,000 m in altitude. Combined with the seismological data described in volume 1 – chapter 4 we use gravity measurements to address the north-south flexural rigidity variations of the Indian plate as it deepens under the Tibetan plateau. Finally, we present the space gravity data acquired over the last two decades to extend the study areas associated with land measurements and to increase the depth of investigation.

5.1. Methods

5.1.1. *Mesurements*

It is well-known that the period of swing T of a simple pendulum is

$$T = 2\pi\sqrt{\frac{L}{g}} \qquad [5.1]$$

where L is the length of the pendulum and g is the local acceleration of gravity [3]. Measurements of the Earth's gravitational acceleration can thus be obtained from the period of a pendulum. During the 17$^{\text{th}}$ and 19$^{\text{th}}$ centuries, more and more sophisticated pendulums were developped and then became the standard instruments of gravimetry.

1. "*To return to the observations made on the Chimborazo, it seems enough to say by closing on the simple fact, that the mountains act in distance, but that their action is much less considerable than the size of their volume promises*"

2. Gravity gradiometry measurements: measurements of the gravity gradient, i.e. the vertical and horizontal variations of the gravity field measured at two points at a known distance.

3. g is ca. 9.81 m.s^{-2} in Paris.

These pioneering gravity measurements allowed significant advances in understanding the shape of the Earth. They also provided the first information on its composition. The 20th century has seen considerable technological advances. Absolute pendulum gravimeters were replaced by free fall gravimeters, in which a tiny weight is let to fall in a vacuum tank and an optical interferometer measures its acceleration. Today, absolute gravity measurements are obtained with a remarkable accuracy of ca. μGal (1 Gal = 10^{-2} m.s^{-2}), which is equivalent to knowing the value of the gravity field with an accuracy of one part per billion!

Absolute measurements are, however, time-consuming and challenging to implement. Therefore, we favor relative gravity measurements carried out in the field by gravimeters that are easier to transport and to handle. The accuracy of relative measurements is ca. 100 μGal, a value that is large enough to detect variations in density associated with geological structures. Most of the data presented in paragraph 5.3 are relative gravity observations acquired in India, along the Himalayan belt, and on the Tibetan plateau. Only a few absolute measurements have been performed to adjust these relative measurements to the previously acquired set of measurements.

Today, the most recent instruments also allow measuring the gradient of the gravity field from airborne or satellite gradiometers. These measurements are expressed in eotvos, in honor of Baron Loránd Eötvös (1848-1919), pioneer of gravity gradiometry measurements. One eotvos represents a variation of one mGal over a distance of ten kilometers. In paragraph 5.4 we will see how these new data sets contribute to the study of Himalayan dynamics.

5.1.2. *Corrections*

Before being used, gravity measurements must be corrected. The first correction is related to instrumental drift. Like many measuring instruments, relative gravimeters drift with time, like a watch that is running a little late or early. Hence, two measurements made at the same location at two different times will not be identical. This drift is estimated from repeated gravity measurements. Assuming that this drift is linear with time and that the time elapsed between each measurement is known, it is possible to correct all measurements carried out in a field campaign. The amplitude of this correction depends on the instrument and can reach up to 0.1 mGal per hour.

Gravity measurements are also sensitive to temporal or spatial variations due to external forcings[4]. Thus the effect of atmospheric pressure changes or tidal deformation of both solid-Earth and ocean-loading must also be corrected (e.g. Longman 1959 ;

4. The term “external forcings” is used to define processes that are not related to the internal dynamics of the Earth

Merrian 1992). Although the amplitude of these corrections is quite small ($\sim$ 0.1 mGal), it is essential to apply them to obtain accurate corrected measurements.

The last corrections are due to the shape of the Earth and its topography. Indeed, any gravity measurement depends on its distance from the center of mass of the Earth (Figure 5.1). Due to its rotation, the Earth is not spherical but ellipsoidal with a polar radius of $\sim 6,357$ km and an equatorial radius of $\sim 6,378$ km. Even with a homogeneous density distribution in its interior, the gravity at the Earth's surface would be greater at the poles than at the equator. Therefore, a latitudinal correction is required to correct the difference in gravitational acceleration as a function of distance from the equator.

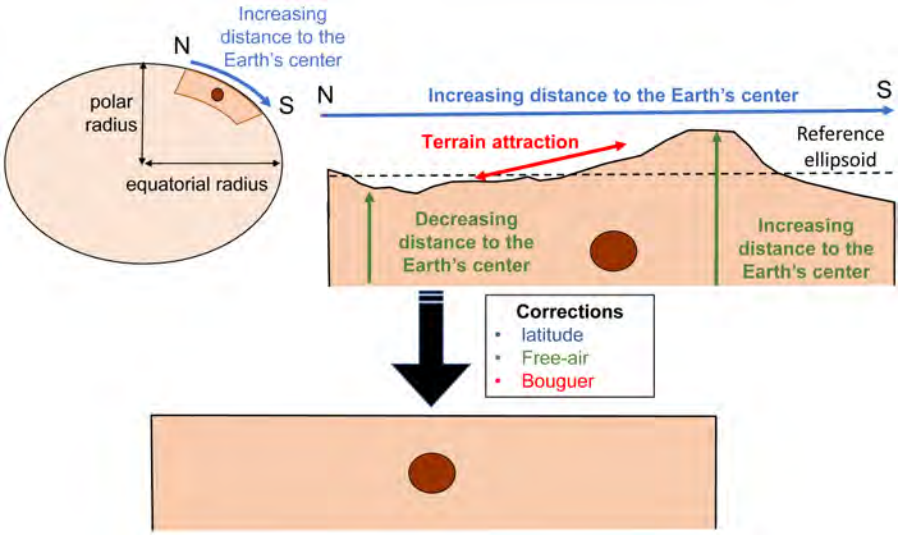

Figure 5.1. *Gravimetric corrections associated with a north-south measurement profile in the northern Hemisphere. The latitudinal correction is related to the ellipsoidal shape of the Earth, which induces an increase in the distance from the center of the Earth for the southernmost measurements. The free-air correction is associated with topographic changes that lead to variations in distance from the Earth's center of mass. The topography also induces mass variations and associated gravity changes, which are taken into account via the Bouguer correction. Applying all these corrections allows studying the reaminig gravity anomalies associated only with density variations at depth. The density is indicated by a color code, which highlights the existence of a density anomaly at depth.*

Moreover, the distance from the center of mass of the Earth depends on the topography. Indeed, at the same latitude, a station located at the top of a mountain is

farther from the center of mass of the Earth than one located at sea level. Therefore, a correction, called "free air correction", must be performed proportionally to the measurement elevation. Finally, a mountain is a massive body. This mass also affects the gravity field. A correction, called "Bouguer correction", is made to take into account this effect. The amplitude of these corrections depends strongly on the measurement elevation. In the case of the Himalayas, where some peaks exceed 8,000 m, these corrections can reach up to several hundred mGal. Therefore, their amplitude can be of the same order of magnitude or even greater than the corrected measurements. It is therefore essential to make these corrections very carefully.

To summuarize, gravity measurements, corrected for instrumental drift and external forcings, must also be corrected for effects associated with latitude and altitude (topography and relief) before any interpretation in terms of density variations at depth can be made (see Dubois et al. 2022, for more details).

5.1.3. *Anomalies*

The corrected observations (measured field minus corrections) are only sensitive to the attraction of massive bodies associated with density anomalies below sea level. They highlight bodies having a density contrast compared to a reference Earth model. "Free air" gravity anomaly is associated with measurements for which latitudinal and free air corrections are applied. "Bouguer anomaly" is the free air anomaly with the extra Bouguer correction. These gravity anomalies can be used over several spatial scales, whether to study a cavity of a few meters, a kilometer-long geological structure or a region such as the Himalayas.

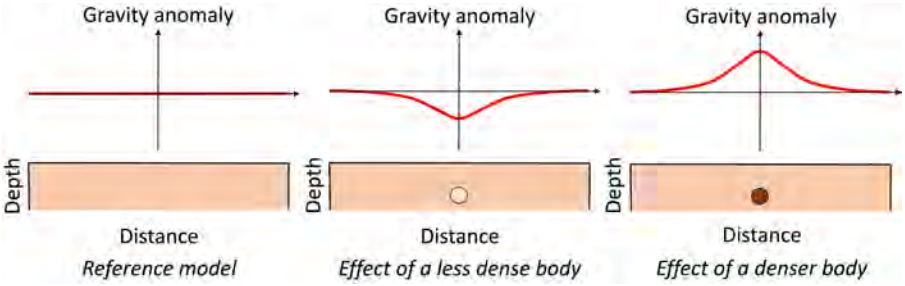

Figure 5.2. *Simplified diagram of a Bouguer anomaly profile associated with a mass deficiency or excess related to a buried sphere with low or high density, respectively. The color code gives the density distribution: light (dark) color = low (high) density.*

A positive Bouguer anomaly is associated with an excess of mass compared to a reference model. In contrast, a negative anomaly is related to a deficiency of mass

below the gravity measurement stations (Figure 5.2). As observed by George Everest, in the Himalayas and Tibet, the negative Bouguer anomaly suggests a mass deficiency below these two regions. The models, allowing to explain this counter-intuitive observation, are presented in the following paragraph.

5.2. Isostasy

Maintaining the high reliefs requires an in-depth understanding of the links between topography and mass distribution. To appreciate this problem, let us return to the work of the French astronomer Pierre Bouguer, who, during an expedition to Peru in 1736-1743, showed that the gravity in the Andes is systematically weaker than at sea level (Bouguer 1749). This study and Everest's observations suggest that the high reliefs are associated with a mass deficiency at depth, compared to the surrounding plains.

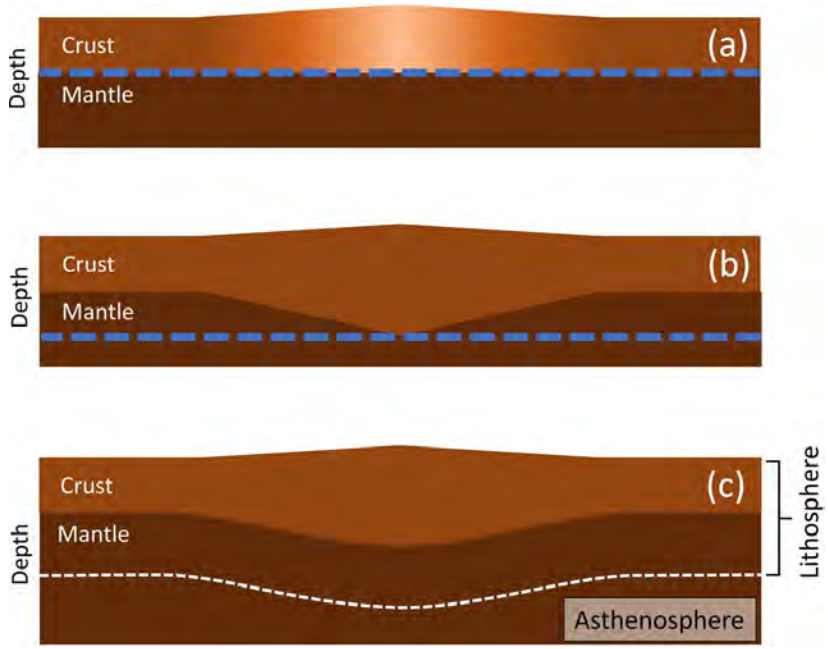

Figure 5.3. *Isostasy compensation models. (a) Local compensation in the Pratt's hypothesis. The dashed blue line corresponds to the compensation depth, i.e. the depth below which all pressures are hydrostatic. (b) Local compensation in the Airy's hypothesis. The dotted blue line corresponds to the compensation depth. (c) Regional compensation provided by the flexure of the lithosphere. The color code gives the density distribution: light (dark) color = low (high) density.*

5.2.1. *Local compensation*

In the second half of the 19th century, two theories of the compensation of the reliefs were proposed to explain the observations made by Everest, then by Pratt (1855) in the Himalayas.

– On one hand, according to John Henry Pratt, the crust under the high reliefs is warmer and therefore less dense than in the adjacent areas (Pratt 1855, 1859). The mass of the topography would thus be locally compensated at depth by a lateral variation of density in the Earth's crust below the topography, without any change in depth of the bottom of the crust (Figure 5.3a).

– For George Biddell Airy, on the other hand, the crust's density does not vary (Airy 1855). Knowing that the crust has a lower density than the mantle, the compensation of the reliefs is then ensured locally by an increase of the crustal thickness (Figure 5.3b).

According to these two assumptions, the pressure exerted below the compensation depth [5] is hydrostatic. The weight of each column of the material above the compensation level is constant. The isostatic compensation is then accomodated locally.

5.2.2. *Regional compensation*

Based on the plate tectonics theory, we now know that the crust and the top-most part of the upper mantle form a relatively rigid layer called the lithosphere. This layer floats on a weak layer that behaves like a visous fluid, the asthenosphere. In Finland, following geodetic surveys showing a systematic uplift of his country, Heiskanen proposed a modification of Airy's model accounting for lithospheric rigidity maintaining the reliefs. Indeed, depending on its rigidity, the lithosphere bends more or less under the weight of the topographic relief, thus distributing the load over a larger or smaller area (Figure 5.3c). This process is called regional isostatic compensation. The landforms are no longer compensated only locally by variations in density or thickness of the crust, but regionally by the rigidity of the lithospheric plates (see Watts 2001, for more details).

In the continental domain, the compensation is mainly ensured by a variation in crustal thickness under a wide plateau (Airy's model) and by the flexure of the lithospheric plate under mountain belts. In the oceanic domain, isostasy can also be accomodated locally or regionally. The oceanic lithosphere is created from hot mantle rock at a ridge. As the lithosphere cools, its density increases; as a result, it subsides (Pratt's model). In subduction zones, the flexure of the lithosphere plays a significant role in the evolution of the arc–deep-sea trench systems.

5. Compensation depth: depth of the crust-mantle boundary in Pratt's model, depth of the thickest crust in Airy's model

Whether the compensation is local or regional, the excess mass at the surface due to the topography is accompanied by a mass deficiency at depth, in agreement with the observations of Pierre Bouguer and George Everest.

5.2.3. *Effective elastic thickness*

The study of the bending of the lithosphere enables the assessment of its elastic properties. Lithospheric rigidity D can be inferred from topographic data and Bouguer anomaly measurements (Figure 5.3b,c). In the case of an non-compensated mountain range, the Bouguer anomaly is zero since no crustal root maintains the relief of mountains. The lithosphere can then be viewed as a highly rigid plate. Conversely, in an area in local isostatic equilibrium, the Bouguer anomaly agrees with gravity associated with Airy's model. In that case, the lithosphere will be regarded as having zero rigidity.

RHEOLOGY OF THE LITHOSPHERE. Rheology is the study of the deformation and flow of matter under the effect of thermo-mechanical stresses. Rheological profiles describe the mechanical behavior of the lithosphere with depth. These profiles involve specific laws (Bayerlee's law, creep law), which define the strength of the lithosphere as a function of depth, and its brittle or ductile behavior. These profiles are obtained from experimental measurements in the laboratory and field observations, including petrological and structural studies, location of seismicity at depth, and joint analysis of gravity anomalies and topography.

The flexural rigidity of the lithosphere varies between 10^{20} and 10^{25} N.m (e.g. Watts 2001). These values are difficult to understand. We, therefore, favor the use of the effective elastic thickness, which corresponds to the thickness of a thin plate with a rigidity D. This thickness h is defined by

$$h = \left(\frac{12D(1-\nu^2)}{E} \right)^{1/3}, \qquad [5.2]$$

where E and ν are the Young's modulus and the Poisson's ratio of the plate material, respectively. In the oceanic domain, the effective elastic thickness is directly correlated to the thermal age of the lithosphere. The older the lithosphere is, the colder it is and the greater its rigidity and equivalent thickness. This thickness then corresponds to the depth of the 450 – 600°C isotherm, which is used to define the base of the oceanic lithosphere. In the continental domain, the physical meaning of this thickness is more complex. The continental lithosphere consists of an upper and lower crust and part of the upper mantle. The associated rigidity is then calculated for a composite plate.

The effective elastic thickness $h_{eff.}$ of the lithosphere is obtained from the elastic thickness of each layer:

$$h_{eff.} = \left(h^3_{upper\ crust} + h^3_{lower\ crust} + h^3_{mantle}\right)^{1/3}. \quad [5.3]$$

Numerical approaches are now available to calculate the deformations associated with topographic loading by considering the distribution of elastic parameters E and ν and the density ρ in the lithosphere. By testing many models with different parameter values, it is, therefore, possible to use $h_{eff.}$ as a parameter to improve the assessment of lithospheric rheology.

5.3. Flexure of the Indian plate

Over the last four decades, numerous research studies have been carried out on the flexure of the Indian plate in context of the India-Asia collision (e.g. Lyon-Caen & Molnar 1983 ; Burov & Watts 2006 ; Hetényi et al. 2006 ; Berthet et al. 2013).

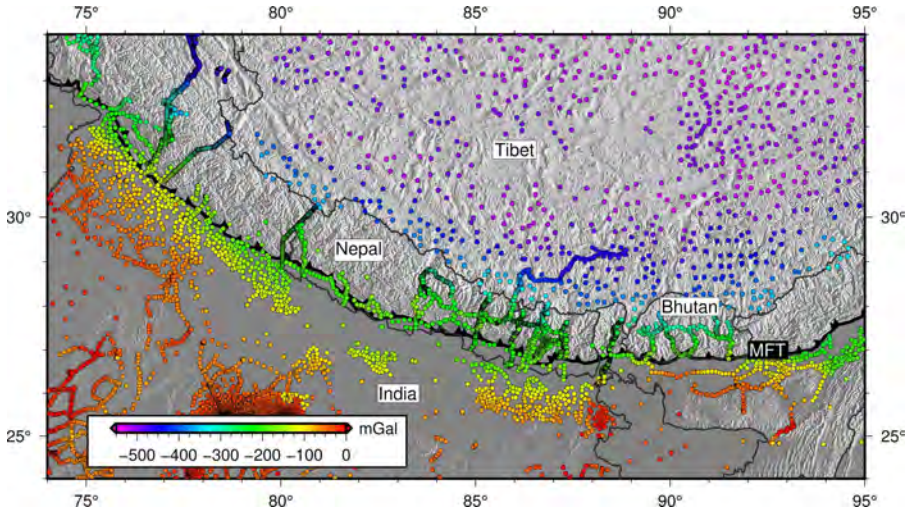

Figure 5.4. *Bouguer anomaly map of the Himalayas and surrounding regions. (e.g. Das et al. 1979 ; Sun 1989 ; Banerjee 1998 ; Martelet et al. 2001 ; Cattin et al. 2001 ; Tiwari et al. 2006 ; Hammer et al. 2013 ; Berthet et al. 2013, Poretti (personnal communication) and the available data from the International Gravimetric Bureau). Color circles give the location of gravity measurements and the associated Bouguer anomaly. Boundaries of countries, geographic regions and the Main Frontal Thrust (MFT) are shown as reference.*

Initially focused on central Nepal, gravity studies showed that the Himalaya were not locally compensated. Part of the load of the highest reliefs had to be maintained by the rigidity of the Indian lithosphere. Since then, several gravimetric measurement campaigns have been carried out to verify this result and test its validity along the entire Himalayan chain.

5.3.1. *Gravity anomaly across the Himalayan belt*

A unique set of land gravity data is now available (Figure 5.4). It consists of about 20 absolute measurements and more than 2,700 relative measurements made in India, Bangladesh, Nepal, Bhutan, and Tibet (see the compilation of Hetényi et al. 2016). The average accuracy of relative measurements is less than 10 mGal. These observations cover more than 2,000 km along the Himalayan arc. They show a strong Bouguer anomaly decrease ($>$ 500 mGal) between India and Tibet. This decrease is localized over a zone, which is 600 km wide, including the northernmost part of the Indian peninsula, the whole Himalayan range, and the southern Tibetan plateau.

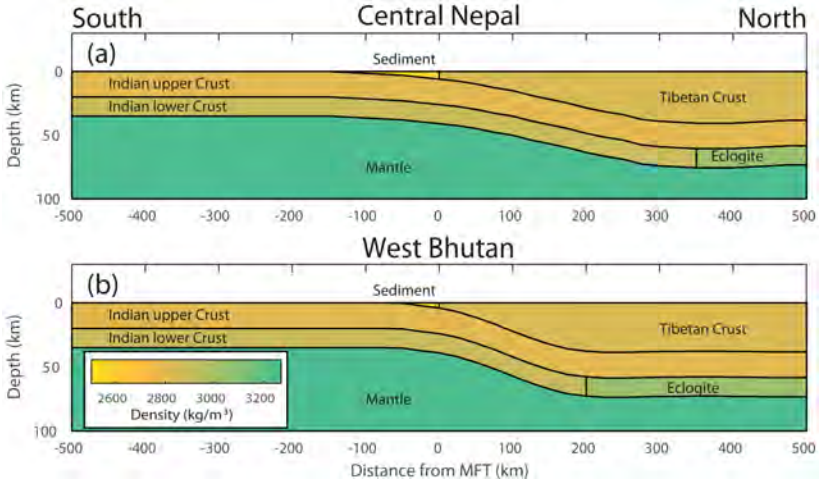

Figure 5.5. *Geometry of lithospheric structures and density distribution across the Himalayan range. These models are obtained from Bouguer anomaly data (Figures 5.4 and 5.6), seismological observations, and borehole measurements across the Himalayas, from India to Tibet. They account for the sedimentary basin associated with the foreland basin, the Tibetan crust and the Indian plate, which is composed of three layers: the upper crust, the lower crust (eclogitized underneath Tibet), and the lithospheric mantle. Distances are given from the Himalayan Frontal Thrust (MFT). (a) Model obtained for central Nepal (Berthet et al. 2013). (b) Model obtained for western Bhutan (Hammer et al. 2013).*

Combined with results from data of seismological networks deployed over the entire region and data from deep boreholes in India, these gravity variations can be associated with (Figure 5.5):

– the foreland sedimentary basin, whose depth can locally reach more than 8 km,

– the flexure of the Indian lithosphere under the Himalayas,

– the local isostatic compensation of the Tibetan plateau by a crustal root with a thickness of ca. 35 km.

Thermo-mechanical models suggest (1) eclogitization of the lower crust beneath the Tibetan Plateau, resulting in its density increase, and (2) north-south variations in the effective elastic thickness of the Indian Plate (e.g., Cattin et al. 2001 ; Hetényi et al. 2006, 2007). The Indian plate is relatively cold before it sinks under the mountain belt. The upper crust, lower crust, and mantle are then strongly coupled, leading to an effective elastic thickness of ca. 70 km. Further north, the deepening of the Indian plate, and the associated heating, lead to a substantial decrease in the crustal rigidity. The effective elastic thickness of the Indian lithosphere is reduced by half to ca. 30 km. The topographic load is then maintained by the rigidity of the Indian lithospheric mantle alone.

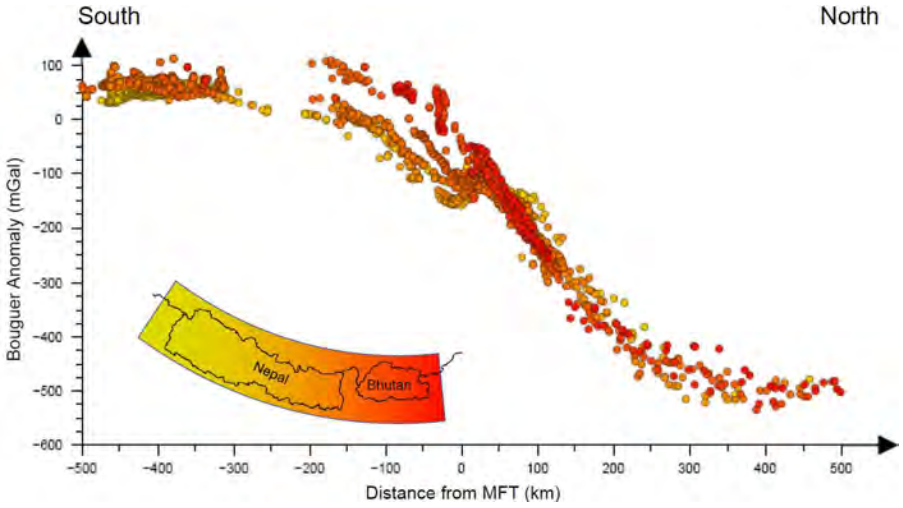

Figure 5.6. *Bouguer anomaly profiles between western Nepal and eastern Bhutan across the Himalayan range, perpendicular to the Main Frontal Thrust (MFT). The color scale indicates the location of the gravity measurements along the Himalayan arc: Yellow, West Nepal - Red, East Bhutan.*

5.3.2. *Along-strike variation between Nepal and Bhutan*

The tectonic units are remarkably continuous along the 2,400 km long arc of the Himalaya. The observed gravity anomalies can therefore be interpreted using two-dimensional models perpendicular to the structures of the Himalayan arc (Berthet et al. 2013). However, a detailed analysis reveals the existence of lateral variations along the Himalaya (Hammer et al. 2013). We focus on the region between central Nepal and eastern Bhutan, where the Bouguer anomaly is well-documented across the mountain belt (Figure 5.4). There we can see the following longitudinal variations in gravity profiles (Figure 5.6):

– South of the frontal thrust, in the foreland basin, the Bouguer anomaly is ca. -300 mGal in Nepal, compared to ca. -100 mGal in Bhutan. This difference suggests a larger and deeper sedimentary basin in southern Nepal than in south of Bhutan (Figure 5.5).

– About 100-200 km north of the frontal thrust, the anomaly is more pronounced in Bhutan than Nepal, suggesting a more rapid deepening of the Indian plate beneath Bhutan compared to Nepal (Figure 5.5).

These along-strike variations can be related to an eastward decrease in the effective elastic thickness from ca. 30 km in Nepal to ca. 20 km in Bhutan. This finding thus suggests strong rheological variations of the Indian plate between Nepal and Bhutan. It is in agreement (1) with seismological studies (see volume 1 – chapter 4) have detected an active fault cutting the Himalayas and the foreland basin between these two areas, the Dhubri-Chungthang fault (Diehl et al. 2017), and (2) with geodetic studies that propose relative motion between the India plate and the block associated with the Shillong Plateau, located east of this fault (e.g. Vernant et al. 2014).

5.4. Satellite data contribution

Land gravity measurements provide valuable information on the geometry and rheology of lithospheric structures. However, field conditions associated with high altitude, limited road network, transboundary issues, and extreme climatic events make the acquisition of these measurements often difficult, sometimes impossible. Thus, many areas such as western Nepal, Himachal Pradesh in the west, or Arunachal Pradesh in the east remain poorly or not surveyed (Figure 5.4). Consequently, the coverage of land measurements remains insufficient to study lateral variations in detail, over the entire Himalayan region.

The first solution is to set up airborne acquisition campaigns. This type of measurement exists for part of Nepal, but these government data are not available to the scientific community. Furthermore, it seems illusory to obtain flight authorizations over territories disputed by India and China. Even then, it would be impossible to get complete coverage because of the steep terrain and flight conditions.

Therefore, the only possibility to complete the land data is to go even higher, using satellite measurements.

5.4.1. *Gravity measurements from space*

The first space measurements of the Earth's gravity field were made in the late 1950s by studying the orbits of artificial satellites. One of the first dedicated campaigns is the GRACE [6] mission launched in 2002. The GRACE mission provided global information on the gravity field and its temporal variations. The method is based on differential acceleration measurements between two satellites flying at an altitude of ca. 400 km. This altitude gives a 600-1,000 km resolution at the Earth's surface, which is still too high to study areas such as the Himalayan arc.

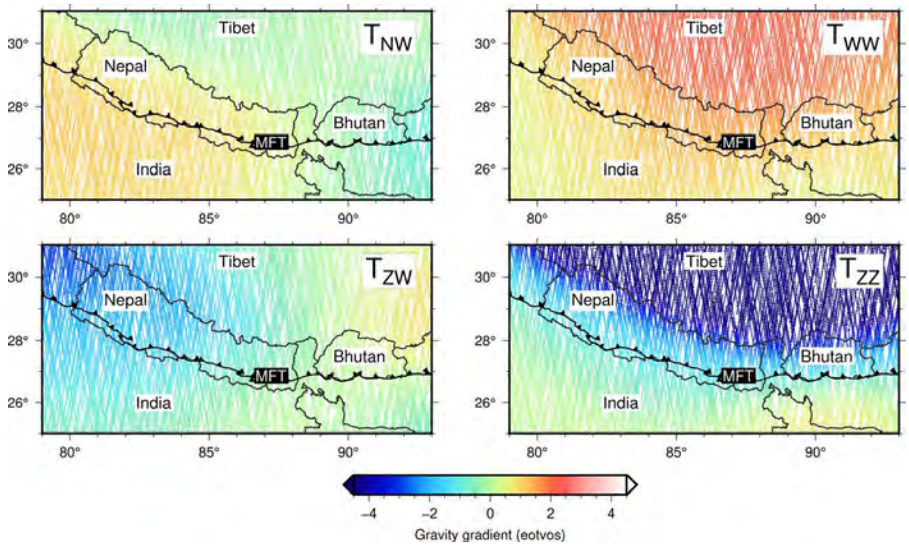

Figure 5.7. *Map of gravity gradients including topographic corrections from the spatial gravity mission GOCE. Color dots represent data along the satellite orbits at an altitude between ca. 225 km and 265 km. T_{ij} is the ij component of gravity gradient tensor. T_{NW}, T_{WW}, and T_{ZW} are associated with the partial derivative of the three gravity components in the west direction. T_{ZZ} is the partial derivative of g_Z in the vertical direction. Borders of countries and the main tectonic structures are shown as reference.*

6. GRACE: Gravity Recovery And Climate Experiment

In 2009, the launch of the GOCE satellite [7] flying at an altitude between 225 km and 265 km has overcome this limitation by yielding a resolution below 100 km on the ground.

On board of the GOCE satellite three perpendicular gradiometers measure the complete gradient tensor T, which is symmetric and its trace is zero:

$$T = \begin{pmatrix} T_{WW} & T_{WN} & T_{WZ} \\ T_{NW} & T_{NN} & T_{NZ} \\ T_{ZW} & T_{ZN} & T_{ZZ} \end{pmatrix} \quad [5.4]$$

where $T_{ij} = \frac{\partial g_i}{\partial x_j}$ with g_i the component of the gravity field in the i direction (W: west; N: north; Z: vertical) and x_j the distance in the j direction. T_{NW}, T_{WW}, et T_{ZW} are the partial derivatives of $\vec{g}(g_N, g_W, g_Z)$ in the west direction. T_{ZZ} is the partial derivative of g_Z in the vertical direction. As previouly mentioned, T is expressed in eotvos [8].

Land gravity measurements and space gravity gradiometry are complementary data. On the one hand, GOCE measurements are sensitive to the three components of the gravity field, while on the ground, only the vertical component is measured. Gravity gradiometry observations better characterize the geometry of anomalies and associated bodies compared to land gravity measurements. The more homogeneous coverage of satellite data also allows a better characterization of the long wavelengths of the gravity field. On the other hand, land measurements are closer to the source of anomalies. They are more sensitive to slight density variations and more relevant to study localized gravity variations.

To maximize the signal-to-noise ratio, we consider the period between August 2012 and September 2013, for which the satellite operated in low orbit at an altitude as low as 224 km. The GOCE dataset consists of 17,500 measurements for the five independent T components from western Nepal to eastern Bhutan. The estimated error is $\sim$ 0.1 E. These measurements show for T_{NW} small variations ($<$ 0.5 E) and for T_{ZW} significant lateral variations (Figure 5.7). In the Tibetan plateau, while positive values (>2.5 E) are observed for T_{WW}, T_{ZZ} exhibits very negative values (<-3.5 E).

5.4.2. *Towards a three-dimensional image ...*

Combined with seismological (e.g. Schulte-Pelkum et al. 2005 ; Nábělek et al. 2009 ; Singer et al. 2017) and land gravity measurements, GOCE data provide an

7. GOCE: Gravity Field ad Steady-State Ocean Circulation Explorer

8. 1 eotvos = 10^{-9} s^{-2}. Its symbol is E.

unprecedented level of detail for imaging lithospheric structures across the Himalayan range.

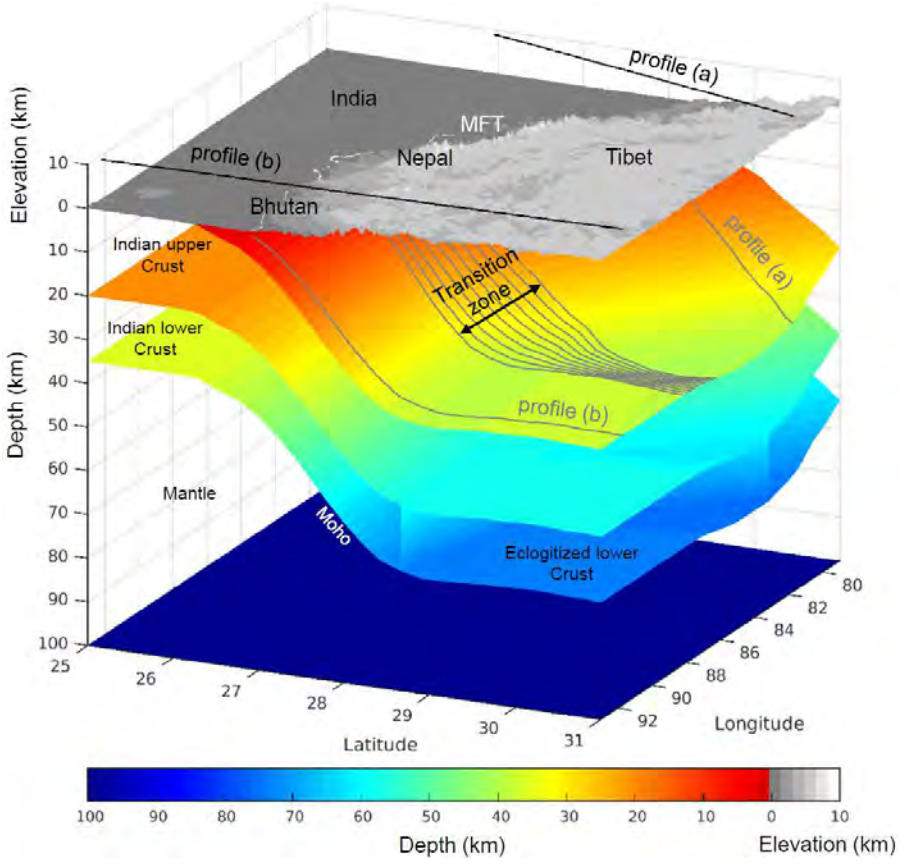

Figure 5.8. *Three-dimensional model showing the geometry of the Indian lithosphere under the Himalayan range and the Tibetan plateau. It is obtained from all available data, including land and space-based gravity observations. Profiles (a) and (b) correspond to two-dimensional models obtained in central Nepal and west Bhutan, respectively (Figure 5.5). The transition zone located at the western boundary of Bhutan is related to an abrupt change in the geometry of the Indian plate. The density distribution is similar to the one used in the two-dimensional models.*

We have shown in section 5.3.2 that the lateral variations observed between Nepal and Bhutan could be associated with a difference in the mechanical behavior of the Indian plate. Here, we use all data sets jointly to better constrain this difference, i.e.

where is the transition zone between the two-dimensional geometries shown in Figure 5.5? What is its width? (Cattin et al. 2021).

The inversion of all land and satellite gravity data provides a three-dimensional image of the lithospheric structures of the region (Figure 5.8). The results suggest a ca. 10 km wide transition, relatively narrow, between Sikkim and Bhutan. This abrupt segmentation is supported by structural observations and could be related to seismically active structures such as the Dhubri-Chungthang fault that cuts the Indian plate beneath the Himalayas. It could be also associated with currently inactive tectonic structures such as the Madhupur fault in the foreland and the Yadong-Gulu rift in southern Tibet.

The obtained transition zone is narrow enough to possibly prevent seismic rupture propagation across this boundary between Nepal and Bhutan. This abrupt geometry could result in the seismic segmentation of the Main Himalayan Thrust and potentially put a higher limit to the size of large earthquakes along the Himalayan arc. These hypotheses now need to be studied in further detail. They could be critical components of future seismic hazard models in this tectonically highly active area.

Conclusion

Since the 19th century, the Himalayas have been an area of pioneering scientific work in studying the Earth's gravity field. The isostasy models of John Henry Pratt and George Biddell Airy, developed to understand the compensation of Himalayan highlands, have been successfully applied to many regions worldwide. Similarly, the concepts of flexural rigidity and effective elastic thickness, used to describe the deformation of the Indian plate, are now commonly used to better characterize the rheology of the lithosphere in both continental and oceanic domains.

Gravity and gradiometry measurements, on the land and from space, are complementary to seismological observations. Together, these data allow us to better image the lithospheric structures associated with the India-Asia collision. In particular, they suggest a complex and three-dimensional geometry of the Himalayan arc with steep segmentations, such as the one located at the western border of Bhutan. These new images are crucial for estimating the seismic hazard of this very active region (e.g., Le Roux-Mallouf et al. 2020 ; Stevens et al. 2020, and volume 3 – chapter 6). Indeed, these transition zones could control the seismic segmentation of the Himalayan range by limiting the size of earthquakes (e.g., Hetényi et al. 2016).

These results are to be confirmed: on the one hand, by increasing the coverage of land measurements, especially in western Nepal, and on the other hand, by improving space observations. Launched in 2018, the GRACE-FO [9] mission aims to characterize

9. GRACE-FO: Gravity Recovery and Climate Experiment Follow-On

the spatio-temporal variations of the gravity field. These data will allow the study of interactions between external and internal forcings in the Himalayan region, where the movement of water masses on the Earth's surface is strongly affected by monsoon cycles. Future gravity field mapping campaigns are underway with innovative absolute gravimeters, which are based on atomic interferometry techniques with cold atoms.

These scientific advances and field investigations will allow us to further improve our knowledge of the Himalayan dynamics, and thus to tackle major societal challenges such as access to water resources and land use planning in this region, where extreme climatic and tectonic events occur.

Bibliography

Airy, G.B. (1855). On the computation of the effect of the attraction of mountain-masses, as disturbing the apparent astronomical latitude of stations in geodetic surveys. Phil. Trans. Roy. Soc. London, 145, 101–104.

Banerjee, P. (1998). Gravity measurements and terrain corrections using a digital terrain model in the NW Himalaya. Comp. Geosci. 24, 1009?1020.

Berthet, T., Hetényi, G., Cattin, R., Sapkota, S.N., Champollion, C., Kandel, T., Doerflinger, E., Drukpa, D., Lechmann, S., Bonnin, M. (2013). Lateral uniformity of India Plate strength over central and eastern Nepal. Geophysical Journal International, 195(3), pp.1481–1493.

Bouguer, P. (1749). La figure de la Terre, déterminée par les observations de messieurs Bouguer et de la Condamine, de l'Académie royale des sciences, envoyés par ordre du roy au Pérou, pour observer aux environs de l'équateur. A Paris: ... Chez Charles-Antoine Jomdert.

Burov, E.B., Watts, A.B. (2006). The long-term strength of continental lithosphere: "jelly sandwich" or "crème brûlée"? GSA Today, 16(1), 4?-10.

Cattin, R., Martelet, G., Henry, P., Avouac, J.P., Diament, M., Shakya, T.R. (2001). Gravity anomalies, crustal structure and thermo-mechanical support of the Himalaya of Central Nepal, Geophys. J. Int., 147(2), 381–392.

Cattin, R., Berthet, T., Hetényi, G., Saraswati, A., Panet, I., Mazzotti, S., Cadio, C. Ferry, M. (2021). Joint inversion of ground gravity data and satellite gravity gradients between Nepal and Bhutan: New insights on structural and seismic segmentation of the Himalayan arc. Physics and Chemistry of the Earth, Parts A/B/C, 123, p.103002.

Das, D., Mehra, G., Rao, K. G. C., Roy, A. L. and Narayana, M. S. (1979). Bouguer, free-air and magnetic anomalies over northwestern Himalaya. Himalayan Geology seminar, Section III, Oil and Natural Gas Resources. Geol. Surv. India Misc. Publ. 41, 141–148.

Diehl, T., Singer, J., Hetényi, G., Grujic, D., Giardini, D., Clinton, J., Kissling, E., GANSSER Working Group (2017). Seismotectonics of Bhutan: Evidence for segmentation of the Eastern Himalayas and link to foreland deformation, Earth Planet. Sci. Lett., 471, 54–64.

Dubois, J., Diament, M., Cogné, J.-P., Moquet, A. (2022). Géophysique, Dunod, pp 272.

Hammer, P., Berthet, T., Hetényi, G., Cattin, R., Drukpa, D., Chophel, J., Lechmann, S., Moigne, N.L., Champollion, C., Doerflinger, E. (2013). Flexure of the India plate underneath the Bhutan Himalaya. Geophysical Research Letters, 40(16), 4225–4230.

Hetényi, G., Cattin, R., Vergne, J., Nábělek, J. (2006). The effective elastic thickness of the India Plate from receiver function imaging, gravity anomalies and thermomechanical modelling, Geophys. J. Int., 167(3), 1106–1118.

Hetényi, G., Cattin, R., Brunet, G., Vergne, J., Bollinger, L., Nábělek, J., Diament, M. (2007). Density distribution of the India plate beneath the Tibetan Plateau: geophysical and petrological constraints on the kinetics of lower-crustal eclogitization, Earth Planet. Sci. Lett., 264, 226–244.

Hetényi, G., Cattin, R., Berthet, T., Le Moigne, N., Chophel, J., Lechmann, S., Hammer, P., Drukpa, D., Sapkota, S.N., Gautier, S., Thinley, K. (2016). Segmentation of the Himalayas as revealed by arc-parallel gravity anomalies. Scientific reports, 6(1), 1–10.

Le Roux-Mallouf, R., Ferry, M., Cattin, R., Ritz, J.F., Drukpa, D., Pelgay, P. (2020). A 2600-year-long paleoseismic record for the Himalayan Main Frontal Thrust (western Bhutan). Solid Earth, 11(6), 2359–2375.

Longman, I. M. (1959). Formulas for computing the tidal acceleration due to the Moon and the Sun. J. Geophys. Res., 64 (12), 2351–2355.

Lyon-Caen, H. & Molnar, P. (1983). Constraints on the structure of the Himalaya from an analysis of gravity anomalies and a flexural model of the lithosphere, J. Geophys. Res., 88, 8171–8191.

Martelet, G., Sailhac, P., Moreau, F., Diament, M. (2001) .Characterization of geological boundaries using 1-D wavelet transform on gravity data: theory and application to the Himalayas. Geophysics 66, 1116?1129.

Merriam, J.B. (1992). Atmospheric pressure and gravity. Geophysical Journal International 109, 231–244.

Nábělek, J., Hetényi, G., Vergne, J., Sapkota, S., Kafle, B.,Jiang, M., Su, H., Chen, J., Huang, B.S. (2009). Underplating in the Himalaya-Tibet collision zone revealed by the Hi-CLIMB experiment, Science, 325(5946), 1371–1374.

Pratt, J.H. (1855). On the attraction of the Himalaya Mountains and of the elevated regions beyond them, upon the plumb line in India, Phil. Trans. Roy. Soc. London, 53–100.

Pratt, J.H. (1859). On the deflection of the plumb-line in India, caused by the attraction of the Himmalaya mountains and of the elevated regions beyond; and its modification by the compensating effect of a deficiency of matter below the mountain mass. Phil. Trans. Roy. Soc. London, 149, 745–796.

Schulte-Pelkum, V., Monsalve, G., Sheehan, A., Pandey, M. R., Sapkota, S., Bilham, R., Wu, F. (2005). Imaging the Indian subcontinent beneath the Himalaya. Nature, 435(7046), 1222–1225.

Singer, J., Kissling, E., Diehl, T., and Hetényi, G. (2017). The underthrusting Indian crust and its role in collision dynamics of the Eastern Himalaya in Bhutan: Insights from receiver function imaging, J. Geophys. Res. Solid Earth, 122, 1152–1178, doi:10.1002/2016JB013337.

Stevens, V.L., De Risi, R., Le Roux-Mallouf, R., Drukpa, D., Hetényi, G. (2020). Seismic hazard and risk in Bhutan, Nat. Hazards, 104, 2339–2367.

Sun, W. (1989). Bouguer Gravity Anomaly Map of the People's Republic of China. Chin. Acad. Geoexploration, Beijing.

Tiwari, V. M., Vyghreswara, R., Mishra, D. C. and Singh, B. (2006). Crustal structure across Sikkim, NE Himalaya from new gravity and magnetic data. Earth Planet. Sci. Lett. 247, 61–69.

Vernant, P., Bilham, R., Szeliga, W., Drukpa, D., Kalita, S., Bhattacharyya, A. K., Gaur, V. K., Pelgay, P., Cattin, R., Berthet, T. (2014). Clockwise rotation of the Brahmaputra Valley relative to India : tectonic convergence in the eastern Himalaya, Naga Hills and Shillong Plateau, J. Geophys. Res., doi:10.1002/2014JB011196.

Watts, A.B. (2001). Isostasy and Flexure of the Lithosphere. Cambridge University Press, pp 458.